

Perspectives on Microfluidics for the Study of
Asphaltenes in Upstream Hydrocarbon Production:
A Minireview

*Mrityunjay K. Sharma and Ryan L. Hartman**

*Department of Chemical and Biomolecular Engineering, NYU Tandon School of Engineering,
Brooklyn, New York, 11201, United States

ABSTRACT

The utilization of microfluidics has generated deep insights into asphaltene precipitation mechanisms and oil-water emulsion stabilization. Agglomeration and precipitation of asphaltenes can cause flow assurance problems during the extraction and transportation of crude oil. Change in temperature, pressure, reservoir conditions, and solvents can change the local environment, leading to asphaltene precipitation. Understanding asphaltene properties and precipitation pathways become critical in devising mitigation methods, demulsifiers, and suitable conditions during hydrocarbon processing. Microfluidics has helped in high throughput measurement studies, understanding critical processing conditions, fast demulsifier screening, the effect of solvent concentration on deposition, generating useful information for the utilization at the point of resource extraction facilitating improved resource management. It has become possible to capture the porous, complex nature of reservoir formations and the interaction of chemicals during precipitation through integrated analytics and visualization studies available only through microfluidics. The use of droplet microfluidics, with optical microscopy and high-speed imaging to study the oil-water interface, has resulted in a greater understanding of the role of asphaltene on interfacial properties and emulsion stabilization. This mini-review highlights the crucial aspects of microfluidics that have been used to understand physicochemical behavior and dynamics of asphaltene deposition. Some of the unique devices have been presented focusing on the key elements of microfluidics design, fabrication, and analysis, as the insight obtained from microfluidics strongly depends on the device design and the controllability of the experimental parameters. Successful implementation of microfluidics for efficient and controlled experiments, short analysis time scales and rapid screening, and generation of high-quality, reliable data that

convey asphaltene deposition issues and interface behavior in emulsion, shows the importance of microsystems for advancing knowledge in hydrocarbon production and processing.

KEYWORDS: Asphaltene, microfluidics, oil-water emulsion, deposition, microfabrication.

1. INTRODUCTION

The heaviest component of crude oil, soluble in aromatics but insoluble in light alkanes, is defined as asphaltene¹. Being the most polar and heaviest component of the crude oil, asphaltenes are also referred to as the "cholesterol of petroleum"². Asphaltenes are one of the few solid components of the crude oil which are challenging to generalize in a particular family since they have different structures³. Generally, asphaltenes are classified as solubility class based on their usual insolubility in light paraffin. Asphaltenes can precipitate or deposit in wellbores, pipelines, and refineries during production and transportation of crude oil and can also stabilize oil in water emulsion, hampering the separation of oil/gas from water⁴. Problems with asphaltene can cost billions worldwide⁵ since the large part of global economy is still dependent on the fossil fuel as a energy source.

Change in the local chemical environment during production and transportation of crude oil, by the change in temperature, pressure, solvent injection for enhanced oil recovery, gas lift operations, and commingling of different crude can change the solubility and solvent power of the medium resulting in the flocculation, aggregation, and precipitation of asphaltenes⁶. In varying geographical locations with differing conditions and compositions of oil wells and temperature, the pressure employed during production/transportation and utilization of different solvent concentrations and composition, optimal flow assurance strongly depends on continuous

monitoring and control of local environment, frequent and accurate characterization of asphaltene behavior and content⁷. Also, developing thermodynamic models describing asphaltene phase behavior are necessary to maintain the conditions at which asphaltenes remain solubilized. Asphaltenes have substantial and irreversible adhesion properties to the solid surfaces, e.g., silica, alumina, and metal surfaces, potentially obstructing the flow in pipeline¹³⁻¹⁵. As sandstone reservoir contains number of oxides e.g. ZrO₂, CaCO₃, TiO₂, SiO₂, MgO, Al₂O₃, and CeO₂, that can affect the aggregation and deposition of asphaltenes¹⁶. Also, studying the interaction between inorganics and asphaltenes becomes crucial for understanding the precipitation, deposition, and mitigation¹⁷.

Asphaltenes can precipitate via multiple pathways, and much of the research is focused on understanding the asphaltene precipitation kinetics, influence of flow environment, interaction with the solvents and inorganic chemical, and effect of varying crude oil composition and production conditions. Conventional asphaltene investigations rely on asphaltene precipitation and the collection of aggregates which helps in predictive modeling of the general behavior of the aggregates, which in terms help in devising the cost-effective mitigation techniques and asphaltene inhibitors¹⁸. In general, asphaltene inhibitors are added to prevent asphaltene precipitation in oil fields which also require lab screening methods before actual application on field¹⁹. Asphaltene inhibitors peptize the asphaltenes and keep them in solution or act on the rock surface to limit the deposition of asphaltenes²⁰. In any case, the inhibitor's effectiveness depends on the structure and chemical nature, the nature of the solvent, dispersion medium, temperature, and pressure during processing^{21, 22}. In general, two types of asphaltene inhibitors are in use, small molecule-based^{23, 24} (e.g., acidic amphiphilic molecules, amides, and imides, ionic liquids, etc.) and polymer-based asphaltene dispersant²⁵⁻²⁷ (e.g., non-polymer alkyls of polymer

polymethacrylate, comb-like polymers, etc.). Salicylic acid, phthalic acid, benzoic acid, dodecyl benzene sulfonic acid, dimethyl amide, polystyrene, maleate co-polymer etc., are being shown to have the effect as asphaltene inhibitors^{20, 28}. Conventional methods of asphaltene content measurement and inhibitor selection utilize a large quantity of solvent, big glass vessels, high temperature, and pressure test methods and require qualified personnel for generating reliable data⁷. Various methods have been developed for studying the asphaltene precipitation and asphaltene deposition in conventional reservoirs, e.g., microscopy²⁹, gravimetric analysis, viscosity measurement³⁰, filtration³¹, electrical conductivity³², light scattering³³, acoustic resonance³⁴, refractive index measurement³⁵, interfacial tension³⁶, heat transfer analysis³⁷, the colloidal instability index³⁸, nuclear magnetic resonance³⁹, and gas chromatography coupled with mass spectrometry⁴⁰, etc. Unavailability of in-situ characterization/measurement techniques, many developed methods, and the very complex nature of asphaltenes, makes understanding asphaltene characteristics difficult and methods by which it can be accurately studied and quantified⁴¹. Also, conditions during experimentation differ significantly from the actual reservoir environment. The results obtained are particular to the crude oil composition, limiting the scope of application in the field.

Microfluidics or lab on chip systems are well developed and utilized in chemical reactions⁴², biotechnology⁴³, diagnostics⁴⁴, nanomaterial synthesis⁴⁵. In the recent decade, microfluidics has gained a lot of importance in asphaltene deposition measurement, in-situ characterization, solvent diffusion, creation of micromodels, etc^{7, 46-49}. The main advantage microfluidics offers is to miniaturize the experimental systems reducing the overall sample volume (microliter to milliliter) and analysis time (seconds to minutes). The integration of inline and in-situ characterization allows the measurement of a large amount of reliable data quickly and in an

automated manner. Microfluidics devices can be fabricated in different materials, e.g., glass, silicon, polymer, metal, or coated with different layers⁵⁰⁻⁶⁵. In addition to the possibility of replication of reservoir porous condition in the microfluidics, utilization of approaches for spatial visualization that combines the optical and spectroscopic techniques makes it possible to extract detailed information about chemical composition and change in physicochemical properties of spatially distributed components. This becomes helpful in terms of observing the dynamic asphaltene deposition with varying chemical and physical environments in the event of agglomeration or precipitation. The recent interest in microfluidics for asphaltene investigation has resulted in the number of microfluidic geometries in different materials to obtain reservoir-like environments by methods such as wettability patterning techniques. The microfluidics devices have been shown to reduce the analysis time significantly compared to the conventional analysis procedures⁷, and measurement related to oil-water interface, composition, phase behavior, and PVT (Pressure-volume-Temperature) properties can be easily performed. While offering a high throughput approach to studying the asphaltene solubility, microfluidics possesses the scale most relevant to natural rock pores (porosity 20 – 40%)⁶⁶⁻⁷⁰ and can be excellent models of porous media^{48, 71}. Microfluidics technology also allows direct measurement of pore scale phenomena, which helps understand the fluid flow properties (oil-water interface, interaction with pore scale, phase composition, gas-oil ratio, and chemical interaction, etc.) in petroleum reservoirs^{49, 72, 73}. In all microfluidics provide well-founded replication of reservoir porous conditions, integration of noninvasive optical/spectroscopic analysis techniques, rapid characterization/ measurement to reduce the labor, and good control over the parameter to study the effect on dissolution, which have helped in understanding the asphaltene aggregation behavior, though they vary on their chemical composition and dependent on the reservoir

conditions. Ultimately microfluidics could yield devices which are easy to deploy in the field and can perform efficient resource management.

This mini-review provides a brief overview of the state of the art of utilizing microfluidics to understand the asphaltene dissolution/precipitation by mimicking similar porous reservoir conditions. Though the literature is flooded with the asphaltene mitigation methods and characterization techniques, those are based on the bulk phenomena, which are quite different from the reservoir conditions. This review focuses on the developed microfluidics designs to study the asphaltene precipitation and the role of asphaltene in oil/gas in water emulsion stabilization. The efficiency of microfluidic platforms and the generation of important knowledge towards asphaltene aggregation and precipitation, which can be implemented in real scenarios, is the focus of this review. General understanding of the factors affecting the asphaltene deposition and their role in microemulsion stabilization done in the microfluidics environment is reported without much quantitative information. For the in-depth details on the experimental microfluidics methods, fabrication of devices, analysis techniques, and obtained results reader is advised to consult the references.

2. ASPHALTENES, THE "CHOLESTEROL OF PETROLEUM"

The main components of crude oil are grouped as "saturates-aromatic-resin-asphaltene" known as SARA. Chromatography is used to determine the composition of crude oil based on the SARA components. Saturates (**figure 1A**) are hydrocarbon compounds that do not contain double bonds, e.g., methane, ethane, etc. As the name suggests, aromatics (**figure 1B**) are the non-polar compounds containing the unsaturated hydrocarbon ring system, e.g., toluene, xylene, etc. The

third component more complex in structure than the first two are resins, which also help stabilize asphaltenes (**figure 1C**). They contain both polar and non-polar components in the structure, helps in stabilizing the non-polar hydrocarbon and polar asphaltenes. Finally, asphaltenes (**figure 1D**) are the polar heaviest component of crude oil, cannot be generalized based on the structure since they have many different structures.

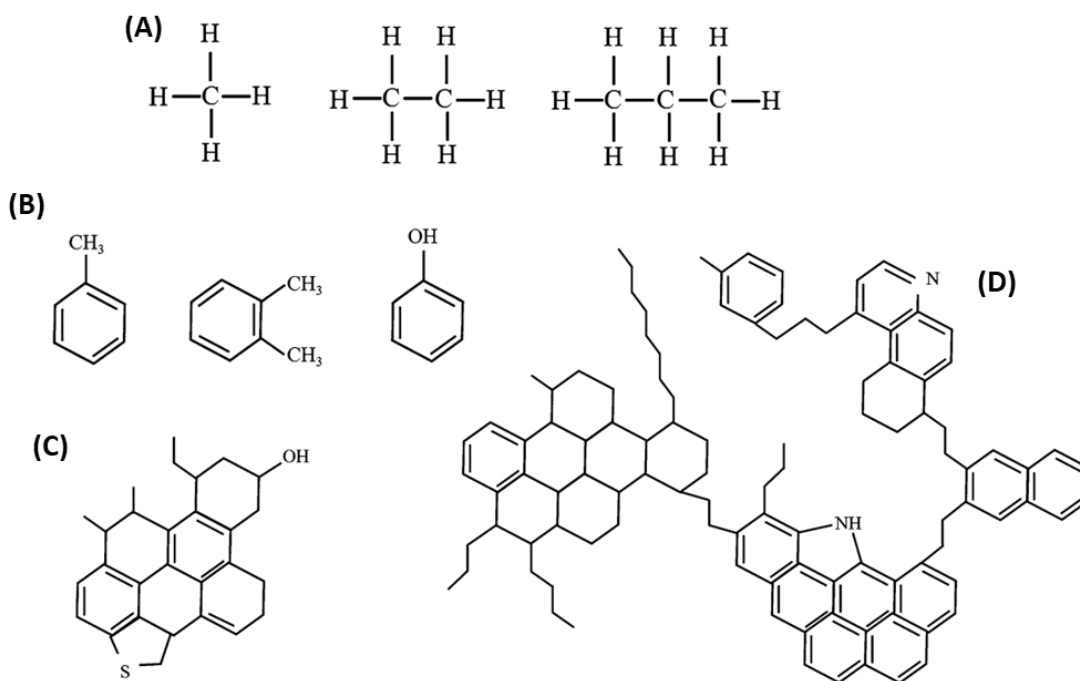


Figure 1. Representative structures of SARA components of crude oil; (A) Saturates; (B) Aromatics; (C) Resin; (D) Asphaltene. Rreproduced from ref 74.

In general, SARA components are separated based on their solubility difference. Initially, crude oil is mixed with liquid propane to isolate the resin, and asphaltene by solubilizing saturates and aromatics. Resin is then separated from asphaltene by solubilizing in *n*-heptane. After isolation, a detailed study on the asphaltene properties can be conducted. **Table 1** lists

some of the previously unresolved issues, which have been clarified with the new and advanced methods in the recent decade; however, the data obtained regarding asphaltene still varies in order of magnitude based on the type of crude and condition prevailing in the reservoir⁷⁶.

Table 1. Issues in reported asphaltene properties values that have been resolved over the past 10 years⁷⁶. Reproduced from ref 65

Issue	Range of reported values	Values (as of 2010)	Distribution width
Asphaltene molecular weight	< 1,000 Da to 1,000,000,000 Da	750 Da	400 – 1,000 FWHM
Number of PAHs in an asphaltene molecule	1 to 20	1 dominates	Small mass fraction with 0, 2, 3, etc., ring systems
Number of fused rings per PAH in asphaltene	2 to 20	7	4–10
Number of PAH stacks in asphaltene nanoaggregate	Unknown	1	—
Aggregation number of nanoaggregates	10–100	<10	4–10
Critical nanoaggregate concentration of asphaltenes	50 mg/liter to 5 g/liter	100 mg/liter	50–150 mg/liter
Concentration of cluster formation	Unknown	~3 g/liter	2–5 g/liter
Size of cluster	Unknown	6 nm for small clusters	Probably larger clusters also depending on

			temperature, concentration
Role of resins in asphaltene nanoaggregate	None to necessary	~15% of crude oil nanoaggregates are resins; resins are not surfactants	Depends on definitions
Relation of nanoaggregate to cluster	Unknown	Clusters consist of nanoaggregates	–
Relation of nanoaggregates in toluene to those in crude oil	Unknown	Very similar in size and composition	–

Abbreviations: FWHM – full width at half maximum; PAH-polycyclic aromatic hydrocarbon

Models describing the method to encompass the possible structure of asphaltenes as a solubility class have been developed. From all the developed models Yen-Mullins model is the most accepted model of asphaltene, which describes the structure of asphaltene based on size and behavior as a function of crude oil in which it is present¹⁸. This model focuses on understanding asphaltene molecule and its presence in crude oil. Methods based on chromatographic separation were used to study the composition of asphaltene in crude oil however, new methods are being developed utilizing the optical and spectroscopic measurement techniques.

Conventional laboratory separation methods are laborious and time-consuming and require skilled operators, whereas optical and spectroscopic techniques are fast and well suited for microfluidics. Many new microfluidics designs with integrated spectroscopic analysis have emerged, contributing to the comprehensive understanding of the asphaltene aggregation and deposition dynamics. The following section will cover some of the unique designs used in the literature in recent years.

3. INNOVATIVE MICROFLUIDIC DESIGNS FOR UNDERSTANDING ASPHALTENE DEPOSITION AND EMULSION STABILIZATION

Though microfluidics provides significant benefits over conventional methods of asphaltene measurements, the real advantage comes from the miniaturization of setup, which offers greater controllability over parameters studied, resulting in noteworthy results in a short analysis time (~30 – 60 minutes). Being small, it is possible to change the process parameters in a fraction of time rapidly. With the advanced measurement techniques, it has become feasible to analyze the whole microfluidic device to get information about the spatial distribution of individual components of the crude oil in the event of precipitation or deposition. A precisely controlled environment helps in generating the stable drop/bubble to study the interfacial phenomena happening during coalescence, which can be visualized in real-time with optical measurement techniques.

Material selection for microfluidics channel fabrication depends on various factors, e.g., property to be analyzed, analysis technique available, final data to be collected, experimental conditions, solvents/reagents to be handled, etc. Based on the fabrication capabilities presented in the literature⁷⁷, there is immense scope of different materials⁷⁸ such as polymer, metal, glass, silicon, etc., which can be utilized for microfluidics chip fabrication. However, fabrication in the glass appears to be the primary material of choice owing to its transparent nature and easy integration with the visualization methods. Though microfluidics reduces the overall experimentation and analysis time, the fabrication procedure is complex, and fabrication time scales are generally of the order of days. Developed fabrication procedures are purely material-

specific, and the resolution quality required at the micron level. However, fabrication procedures have been standardized over the years, and commercial manufacturers are also available in the market to satisfy the need of novice researchers who only want to utilize the power of microfluidics for their research without going much into the details of fabrication. **Table 2** provides the list of innovative microfluidics designs fabricated to understand deposition dynamics of asphaltene in crude oil.

An initial report of utilizing microfluidics in heavy oil extraction is based on a simple H-cell design (**figure 2.3**) fabricated on microscopic glass slides using wet-etching technique⁷⁹. Hexane and hydrocarbon samples were pumped into the H-cell in a co-current manner and extracted polar and non-polar fractions were collected at the outlet for analysis on Gas Chromatograph. The same H-cell was used to extract carboxylic content from the heavy oil to study the asphaltene content⁸⁰. However, diffusion-based separation works only at microscales, possible only in microdevices that were later shown to be applicable for separating other components of the crude oil and analysis⁸¹. Simple geometry and rapid extraction demonstrated the possibility of tremendous applications of microfluidics in crude oil composition analysis where immediate measurement of small samples is required. In a recent simplistic approach, 100-micron microcapillary was used to study the dynamics of asphaltene deposition at various flow rates and change in asphaltene concentration in capillary flow utilizing the power of microfluidics and avoiding the extensive fabrication procedure⁸².

Table 2. List of microfluidic devices used for studying the deposition of asphaltenes

Device	Dimension	Material and fabrication method	Analytics	Utilization	Insight
2D Micromodel ⁷¹	Length 10 cm; Width 10 cm; Depth 57 μm	In glass using photolithography and wet etching	Optical and thermal imaging	For the understanding pore-scale mechanism of steam solvent coinjection; mapping the condensate zone and steam solvent coinjection temperature	Steam solvent coinjection depends on azeotropic temperature, saturation temperature, degree of dilution, and asphaltene deposition in the condensate phase
Microfluidic cavity with IR cell ⁶	Channel thickness 100 μm ; width 2.5 mm; cavity width 5 mm	Third-party fabricated in glass with CaF2 window	Fourier transformed infrared spectroscopy	To observe the spatial distribution of components during the formation of aggregates	The flow of heptane leads to non-ideal conditions reaching beyond the threshold for asphaltene deposition; fast asphaltene aggregation result is firmly fixed deposits on the surface
2D microfluidics ⁸³	260 μm side channel; 20 μm main channel	In borofloat glass using photolithography and wet etching	Internal reflection microscopy	For in-situ observation of phase separation	It is possible to remove scattering of subphases, and diffusive mixing can be controlled in the microfluidics
Microfluidic chip ^{5, 7}	Mixer – 125 μm \times 350 μm ; small channels 50 μm \times 125 μm ; Reactor 250 μm \times 370 μm ; inlet and	In glass using lithography, isotropic etching, and	Light source and UV-visible spectroscopy	To measure asphaltene content in crude oil; evaluate the solubility of crude oil asphaltenes; to make automated microfluidic setup for	Microfluidics with integrated analytics can be applied to high throughput screening; asphaltene content measurement can be done in less than 30 min

	interconnecting channels 175 μm \times 350 μm ; filtration channel 200 μm \times 600 μm ;	temperature annealing		measuring asphaltene yield	compared to days using conventional techniques; measuring the solubility of asphaltene is easily feasible in crude oil
micro packed bed ^{17, 46, 84-86}	triangular geometry 9.9 μL ; rectangle 48 μL ; (μ pillars; 30 rows \times 250 columns) 20 μm diameter; 20 μm pillar-to-pillar distance	In glass and silicon using photolithography and deep reactive ion etching	UV-visible spectroscopy; Raman spectroscopy; Pressure measurements	To mimic the porous reservoir properties; to evaluate the effect of aluminosilicate	Alumina content delays the asphaltene nano aggregation and has higher susceptibility towards bigger molecules; high temperature helps in easy removal of asphaltenes;
microfluidics cell ⁸⁷	Feeding and exit channel 300 μm and 2 mm; height 60 μm ; The flow-focusing orifice width 50 μm	In polymerized and cured PDMS using soft lithography	Optical microscopy using a high-speed camera	To study electro-coalescence of aqueous droplets in crude oil	With microfluidics, electrostatic forces driving the coalescence can be calculated precisely to predict the onset of the coalescence event
microfluidics flow-focusing device ^{88, 89}	Height 20 μm	In PDMS bonded on glass using standard lithography and soft lithography		To screen the evolution of crude oil-brine interface elasticity	Using low salinity brines reduces the crude oil snap-off, which enhances the oil recovery; asphaltene in crude oil aids in the development of elastic film, which depends on the concentration and composition of brine and crude oil

microcapillary ⁸²	Length 10 cm; Width 100 μm	Commercially available borosilicate glass square microcapillaries	Optical microscopy with high-speed imaging	to study the impact of flow rate and concentration of precipitant on dynamics of asphaltene precipitation	The size of asphaltene deposits depends on the elapsed time, and size distribution becomes wider at higher precipitation concentration
micromodel ⁹⁰	Length 9 cm; Width 1.5 cm; Throat width 110 μm ; Throat depth 100 μm ; Matrix 0.14 \times 10- 3 m	In glass fabricated from third party manufacturer	Optical microscopy with high-speed imaging	to study the pore throat plugging and snowball effect	Pore plugging behavior varies based on the initial and middle stage of deposition
porous media microfluidics ⁹¹⁻⁹³	Length 4 cm; Width 0.41 cm; Height 15 μm	In NOA 81 (Norland optical adhesive)	Optical microscopy with high-speed imaging	asphaltene remediation via microemulsion formulation; Characterization of asphaltene in the presence of chemical dispersant	Asphaltene removal strongly depends on the amount and type of solvent contained in the microemulsion
H cell microfluidics ⁷⁹⁻⁸¹		In glass	Offline GC analysis	Rapid extraction of different components from crude oil	Components of crude oil can be extracted easily using microfluidics in a short time
Pore throat model ⁴⁷	circular posts depth = 100 μm ; pore body width 100 (\pm 1) μm ; pore throat width 40 (\pm 1) μm ; depth 15 (\pm 1) μm	In glass using standard lithography and wet etching	Helium ion microscopy; Total internal reflection microscopy	To evaluate the deposition of asphaltene in the solvent-based extraction process	Asphaltene precipitation with n-decane forms large particles while smaller particles precipitation with n-pentane leads to higher aggregation and flocculation

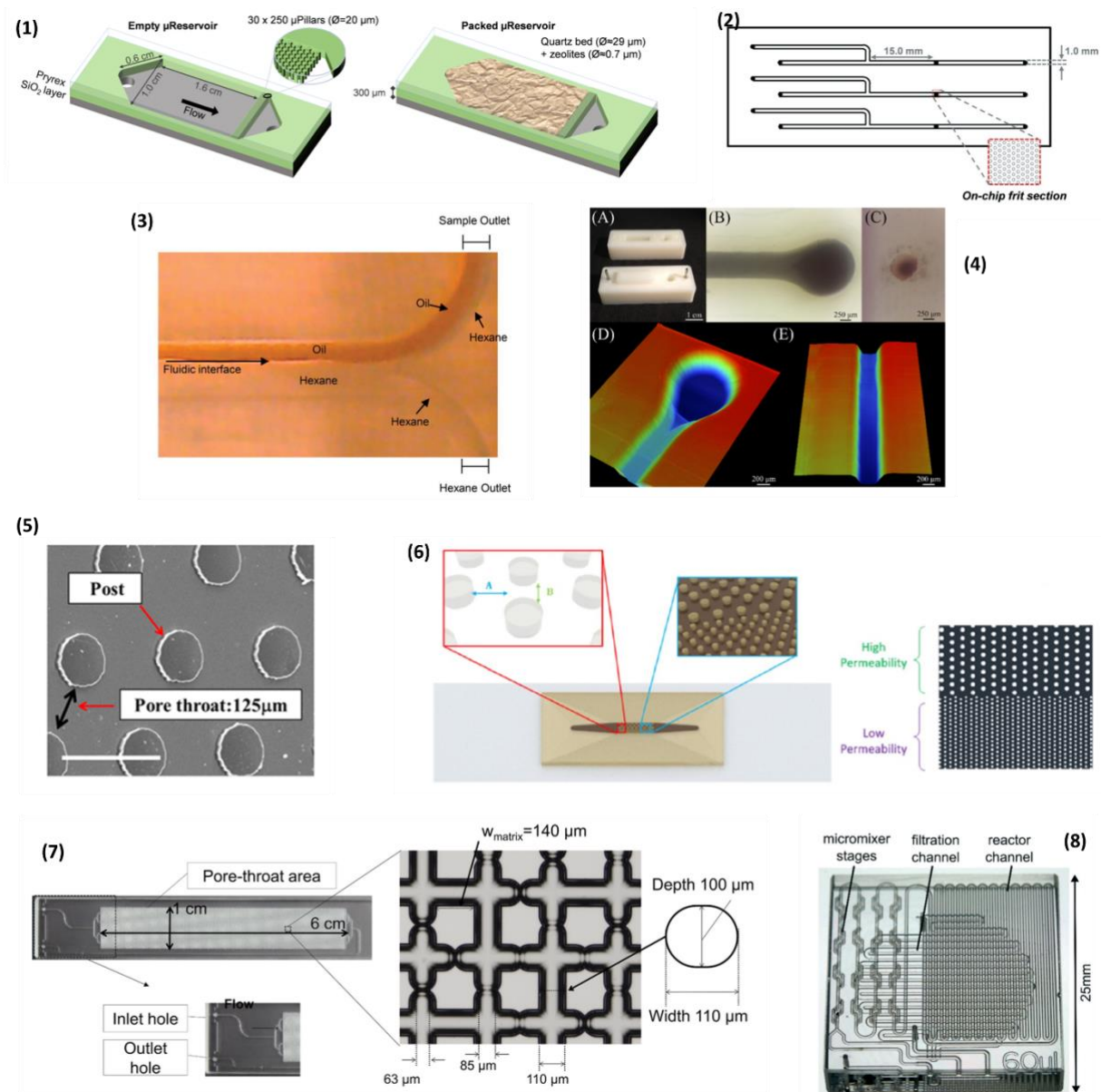


Figure 2. Microfluidics designs for understanding the asphaltene deposition; (1) μ -Reservoir (Pyrex/ SiO_2) design specifications and its states: empty (left side) and packed (right side). Reprinted with permission from ref. ¹⁷. Copyright 2017 American Chemical Society; (2) 2D design of the automated packed-bed microreactor (AUTO3- μ PBR); (3) Image of H-cell device in operation. Contact labeled as the interface between the two fluids and the fluids exiting the device. Reprinted with permission from ref. ⁸¹. Copyright 2014 Royal Society of Chemistry; (4)

Characterization and surface depth profiles of a 3D-printed μ -SPE system for sample preparation of crude oil. (4-A) The microfluidic device showcasing the base component (top) and assembled device (bottom). This device comprises a cylindrical sample compartment and a rectangular container for the stationary phase. Dimensions of microchips are 25 mm \times 50 mm of base and 10 mm of height. (4-B) Photos by digital stereoscope of microchannels, highlighting half-printed microchannel. (4-C) cross-section view of the approximately circular channel. Dyes were used to enhancing visualization. (4-D) Profilometry of the half-printed base component of μ -SPE output.(4-E) microfluidic channel. Reprinted with permission from ref.⁹⁴. Copyright 2017 American Chemical Society; (5) SEM image of the porous media used to study deposition. Reprinted with permission from ref.⁹¹. Copyright 2017 American Chemical Society; (6) Illustration of a dual-permeability porous media microfluidic device. (A) and (B) indicate the distance between horizontal and vertical pillars, respectively. Reprinted with permission from ref.⁹³. Copyright 2021 American Chemical Society; (7) The appearance and (b) a lattice-like structure of the pore-throat area and the cross-sectional shape of the throats of the micromodel. Reprinted with permission from ref.⁹⁰. Copyright 2021 Elsevier; (8) Core microfluidic chip: photograph of an empty glass chip containing the mixer, reactor, and filter channels. Reprinted with permission from ref.⁵. Copyright 2015 Royal Society of Chemistry.

Fabrication in glass and silicon needs specific procedures to be followed in succession and requires cleanroom facilities. In general, fabrication steps involve surface cleaning, metal layer deposition, photolithography, wet and dry etching with several heat treatment steps, and finally, removal of deposited metal layers from wafers. Once desired quality and dimension of channels are obtained, the wafers can be bonded together to get the microfluidic device. The detailed

fabrication procedure can be found elsewhere⁹⁵. The enormous success of microfluidics in asphaltene deposition goes to the ability to mimic the similar porous structure (porosity) found in the reservoir rocks with the help of either packing material⁴⁶ or fabricating the pillar⁴⁸ structure inside a microfluidic channel where precipitation and pore interactions can be studied simultaneously.

To study the deposition of asphaltenes in the porous media and to mimic the reservoir conditions, a microfluidic chip packed with porous quartz media (**figure 2.1-2.2**) was fabricated⁴⁶. Initially, the triangular design and frit section at the outlet was formed in silicon using dry reactive ion etching (standard silicon chip fabrication procedure), then anodically bonded to the Pyrex glass top. After fabrication, crushed and carefully sieved quartz particles were manually injected inside the chip to form a μ -packed bed. In another approach, a pore throat structure was created in a glass microfluidic device to study the effect of deposition in the pore throat (**figure 2.7**) of the reservoir rocks. Inlet, outlet and the pore-throat area were formed by lattice-like structure on the micromodel⁹⁰, and to induce inhomogeneous streamlines of flow, parts of the throat area were randomly curved.

Moving away from glass microfluidics, Lin et al. fabricated a microfluidic device (**figure 2.5-2.6**) using Norland Optical Adhesive (NOA-81) to study the effect of different microemulsion and their impact on the removal of asphaltene deposits⁹¹. This design employed the posted/pillar arrangement in the flow path to mimic the porosity. However, to change the permeability, the size and density of the micropillars were varied, keeping the same porosity. In a similar approach, the micromodel with a homogeneous two-dimensional porous network of circular posts with pore-throat size close to the natural oil sand porous media was fabricated in the glass. In this design, only the pattern/ arrangement of posts was changed in two forms to study the

deposition of asphaltenes during solvent-based extraction of bitumen⁴⁷. Also, Silane treatment was applied to porous media to measure the effect of wettability alteration on asphaltene deposition. In an ideal environment with uniform structure micromodel effect of parameters like pore geometry, tortuosity and other parameters can be easily studied.

In an independent approach to circumvent the lengthy and laborious fabrication procedure in glass and silicon devices, a 3D printed microfluidics (**figure 2.4**) system was proposed and developed for solid-phase extraction. Fused deposition modeling via a 3D printer was used, and a microdevice was fabricated in polylactic acid (PLA) substrate⁹⁴. It is easy to fabricate complex structures in polymer microfluidics using 3D printers (as they are easily accessible), but it restricts the usage only to some compatible solvents. The swelling of material in a non-polar solvent and the integration of functional 3D elements in the microfluidics platform were two essential considerations behind this fabrication. It was observed that the microfeatures remained fully functional even after 20 min of exposure to the non-polar solvents. This can be beneficial in terms of a disposable device used for single analysis or extraction; however, it cannot be used for operations where prolonged use is desired.

Microfluidics is also used to study the role of asphaltene in oil-water emulsion stabilization. In these studies, the designs are primarily straight channel type where generation and monitoring of droplets throughout flow path becomes feasible through optical measurement techniques. In most cases, the droplets are generated in different flow environments, and the effect on droplet coalescence was observed by changing the parameters, generally the addition of an emulsifier or inhibitor (**Figure 3**). In these experiments, the quality of the data depends on visualization techniques, primarily using a high-speed camera to take images over the entire flow path and at a different time to observe the dynamics during the flow. As the success of these devices rests on

the ability to monitor the phenomena happening inside, devices are made chiefly of glass; however, it is difficult to segregate between the device solely used for asphaltene deposition studies and emulsion characterization. Some important microfluidic devices used for studying the oil-water emulsion are listed in **table 3** and in **figure 3**.

In a simple method to determine the effective demulsifier based on observation of drop coalescence, a simple 500 microns square capillary was used⁹⁶. The capillary was connected to the drop generation system and the capillary was irradiated with a near-infrared laser, and images were taken using a high-speed camera. Coalescence probability was determined based on visual observation, sufficient for quantifying an effective demulsifier. Hu et al. used the same micro-packed bed device (**figure 2.1**) to study the effect of asphaltene concentration on the heptol brine interphase and the fluid-fluid interphase was characterized with inline analytics⁸⁴. A commercially available droplet generation chip (**figure 3.1**) was utilized to study the effect of additives on the separation behavior of water in diluted bitumen emulsion⁹⁷. Different additives were added to the emulsion in one experiment, and the kinetics of droplet coalescence were measured, in contrast, in another experiment, droplets in the emulsion were aged first, and then additives were added and the coalescence rate was observed. A custom-designed glass microfluidics chip (**figure 3.3**) was used to study the attachment of crude oil drops to the gas bubbles⁹⁸. Microfluidics-based methods (**figure 3.2**) help understand the effect of oil, water, and gas phases on the attachment of oil droplets to the gas bubbles. The same setup was also used for studying the coalescence of crude oil drops in water to check the effect of oil/water composition and the aging of the droplets⁹⁹.

Moving away from glass microfluidics, the device made using NOA 81 (Norland Optical Adhesive), a thiolene photopolymer (**figure 3.4**) with known solvent resistance and temperature

tolerance, was used to study the effect of different demulsifier and their concentrations⁴⁸. Also, the emulsion stabilization characteristic of fractionated asphaltenes and the two model molecules coronene and violanthrone-79 with flow-focusing was studied in the same device⁹². The generation of stable droplets depends on the surface properties and the droplet braking dynamics, and it is necessary that in each experiment, surface properties remain the same, which requires good cleaning of the device after each investigation or after a specific duration of using it.

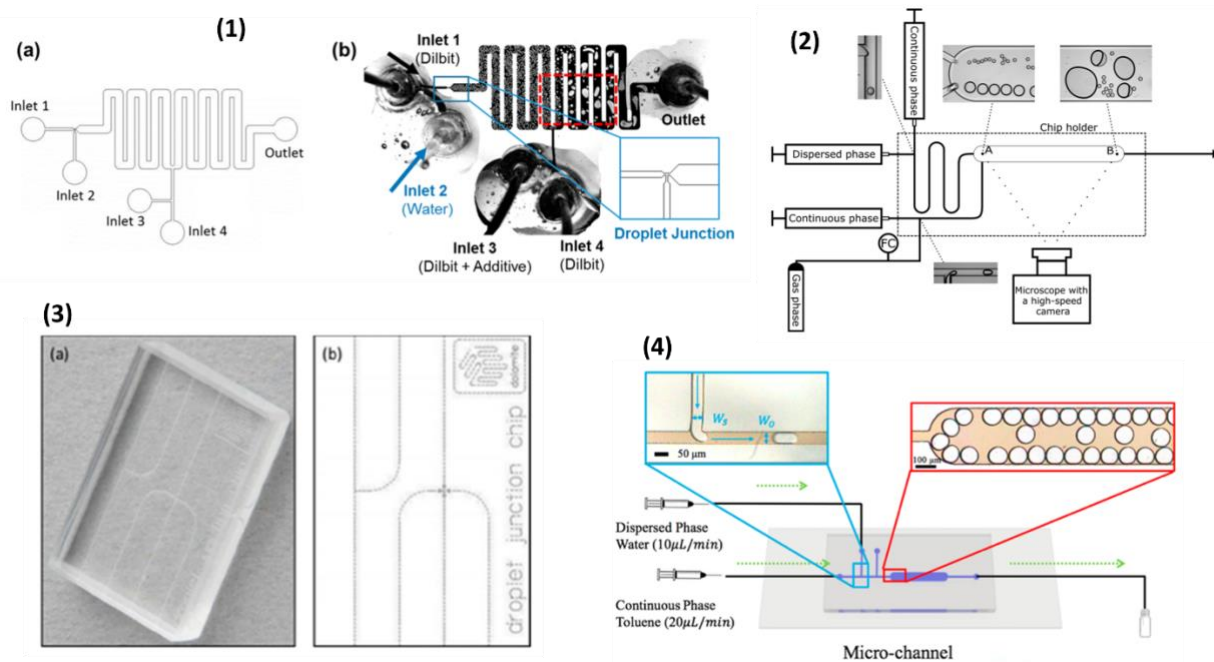


Figure 3. (1) (a) Schematic of a microfluidic device for aging droplets before introducing additive. The width of the serpentine channel was $1000\ \mu\text{m}$ with a constriction to $100\ \mu\text{m}$ at inlets 3 and 4. (b) Photograph of the device with water droplets being generated in dilbit. The droplets only coalesced after the additive was introduced. The dashed red box outlines the field of view imaged during the experiments. Reprinted with permission from ref.⁹⁷. Copyright 2017 American Chemical Society; (2) Microfluidic setup and chips. Droplets and bubbles, generated at two T-

junctions, enter a wider channel (point A) and interact with each other, leading to the attachment of some freely flowing drops to bubbles at the end of the channel (point B). Reprinted with permission from ref.⁹⁸. Copyright 2018 American Chemical Society; (3) (a) Droplet generation chip (b) schematic of the chip showing the flow channels. Reprinted with permission from ref.¹⁰⁰. Copyright 2017 Elsevier; (4) Schematic of the microfluidic experimental setup for emulsion stabilization characteristics of asphaltene. Reprinted with permission from ref.⁹². Copyright 2020 American Chemical Society.

Table 3 List of microfluidics devices used for studying the oil-water emulsion

Device	Dimension	Material and fabrication method	Analytics	Utilization	Insight
Microfluidic chip 1¹⁰¹	Solvent channel width 50 μm ; depth 20 μm ; bitumen-solvent PVT channel width 50 μm ; depth 20 μm ; bitumen channel width 5 μm ; depth 5 μm	In glass and silicon using deep reactive ion etching and shadow mask process	Optical microscopy with high-speed imaging	For measurement of solubility and diffusion coefficient of propane in bitumen	Fast quantification, small sample volume, ease of operation at high temperature and pressure; with 1nl volume microfluidics require less than 1 hour, which is 150 times faster than convention method, which takes 7 days
Microfluidic chip 2¹⁰⁰	Channel cross-section at junction depth 100 μm ; width 105 μm ; Wide channel cross-section depth 100 μm ; width 300 μm ; Channel length after junction 11.25 mm	In glass standard lithography and wet etching	Optical microscopy with high-speed imaging	For emulsion characterization with different solvents and effect of salt	The type and concentration of inorganic salts used have a negligible impact on the droplet size of the emulsion
microcapillary based⁹⁶	Length 300 mm; width 500 \times 500 μm	Commercially available glass microcapillary	Optical microscopy with high-	To test demulsifier enhancement of coalescence-rate of	Coalescence probability can be quantified by observing the

			speed imaging	water droplets in crude oil	monodispersed droplets and changes in their size
microfluidic chip 3⁹⁷		In Norland Optical Adhesive (NOA) 81 using soft lithography	Optical microscopy with high-speed imaging	Water Droplet Coalescence and Flocculation in diluted Bitumen Emulsions with Additives	Effectiveness of the different additives can be characterized by observing the coalescence time
Microfluidics chip 4⁹¹	Channel width 100 μm ; collision chamber width 500 μm ; Channel height 50 μm .	In Norland Optical Adhesive (NOA) 81 using soft lithography	Optical microscopy with high-speed imaging	To study emulsion stabilization via asphaltene	The state of aggregation of asphaltene strongly affect the stability of the emulsion

4. AUTOMATION OF MICROFLUIDICS WITH ANALYTICAL METHODS FOR ASPHALTENE MEASUREMENTS

The overall setup in the microfluidics experiment remains the same except for different microfluidic chips and integrated analysis techniques. The general schematic of the whole experimental setup is shown in **figure 4**³⁰.

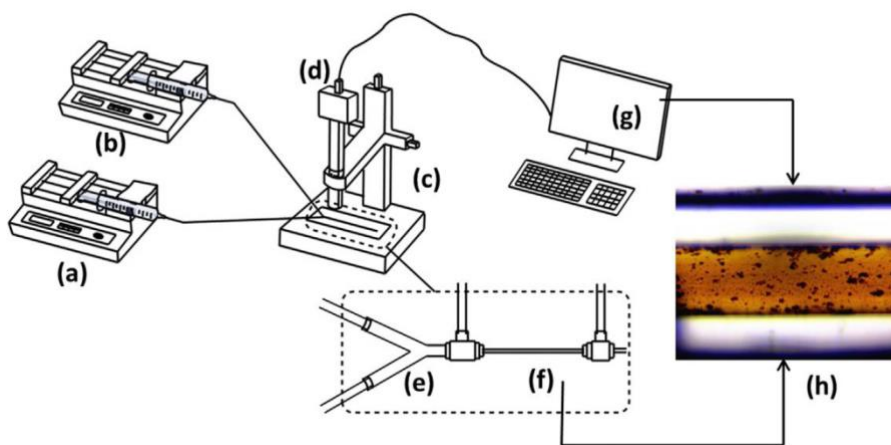


Figure 4. Experimental setup for asphaltene deposition experiment in capillary flow⁸²; (a) constant-flowrate microfluidic pump A, (b) constant-flowrate microfluidic pump B, (c) microscope, (d) high-speed digital camera, (e) Y-connector, (f) microcapillary, (g) data acquisition computer, (h) microscopic image of asphaltene deposits in capillary flow. Reprinted with permission from ref.³⁰. Copyright 2018 Elsevier.

A good analysis/measurement technique integrated with microfluidics provides tremendous scope for collecting valuable data. In the case of asphaltene, an integrated analytical instrument depends explicitly on the asphaltene property under investigation and the nature of the data to be collected. Over the years, different methods used for asphaltene characterization can be categorized based on property under focus, such as Gravimetric methods, density measurements,

optical microscopy, light scattering, and refractive index measurements. Compared to density and gravimetric methods, other methods can be directly integrated with the microfluidic platform to generate the specific information in real-time. Analytical instruments have been employed, e.g., FTIR⁶, total internal reflection microscopy⁸³, optical microscopy⁷, Raman spectroscopy⁴⁶, etc., to study the asphaltene. **Table 4** lists some of the utilized analytical techniques for measuring and monitoring the asphaltene properties and behavior which can be potential drivers for the high throughput analysis in short time. Large amount of data generated using these techniques can fuel the development of Artificial Intelligence and Machine Learning based approached which can further help in advancement of the field.

Table 4. Analysis techniques used for asphaltene measurements for high throughput screening that can fuel the data requirement for machine learning and artificial intelligence approaches.

Analysis	Utilization
Nuclear magnetic resonance spectroscopy ¹⁰²⁻¹⁰⁶	For asphaltene chemical structure characterization, molecular interaction between asphaltenes and maltenes, dynamic behavior of asphaltene in bulk and confinement
Fourier transform infrared spectroscopy ¹⁰⁷⁻¹⁰⁹	Measurement of the spatial distribution of chemical component and their amount; Display of process of aggregate formation
Total internal reflection microscopy ^{83, 110}	For in-situ observation of precipitation and phase separation; high spatiotemporal study of precipitation dynamics for asphaltene deposition
Optical absorption spectroscopy ^{29, 111-113}	Used for determination of asphaltene weight content in crude oil based on absorbance difference; asphaltene yield measurement
Raman spectroscopy ^{17, 85, 86}	For 2D and 3D mapping of the whole microfluidics chip to give insights about asphaltene sheet size and bed occupancy
Optical microscopy with high-speed imaging ^{47, 48, 93}	For visualization of asphaltene deposition dynamics; oil-water emulsion interface characterization; Understanding the role of asphaltene in emulsion stabilization

FTIR with an array of detectors allowed the spatial resolution of chemical components and their composition during aggregate formation⁶. In contrast, total internal reflection microscopy removes the effect of scattering from subphases in the mixture with high-quality spatial and temporal resolution⁸³. Raman scattering was used to determine the chemical interaction and get insights into the asphaltene sheet size and bed occupancy during the deposition⁴⁶. Optical imaging at droplet level study can generate useful information so that electrostatic forces driving the droplet merging can be calculated and the coalescence event can be predicted. The asphaltene coloration can be directly correlated with asphaltene weight content which can be helpful in real-time analysis using optical absorption techniques⁷.

Integration of optical microscopy and absorbance spectroscopy in microfluidics can result in rapid analysis and measurement of different components of crude oil. On this principle, researchers have shown that high throughput screening can be employed at the point of resource extraction or in the laboratory, reducing the analysis time from days to hours. It was shown that a simple H-cell microfluidics could extract the hydrocarbons from the crude oil quickly, which can be analyzed on Gas Chromatograph⁷⁹. Later, it was shown that the same H-cell was efficient for extraction of asphaltene⁷⁹, carboxylic acid⁸⁰, determination of the total acid number⁸¹, etc. Continuing on the same lines, a microfluidic device integrated with absorbance spectroscopy was developed where the difference between the initial absorbance of crude oil and absorbance after precipitation of asphaltene was correlated with the asphaltene weight²⁹. This simple approach can be utilized for rapid determination of asphaltene content of the crude oil based on precipitation and separation^{5, 7}.

Asphaltenes affect the oil recovery through alteration of wettability and blockage. Asphaltene precipitation depends on various parameters, e.g., fluid properties, reservoir conditions, pressure,

temperature, dilution ratio, injected fluid molecular weight, etc. It is pretty challenging to apply predictive ability based on the generated data using inline/real-time measurement techniques via conventional thermodynamic¹¹⁴⁻¹¹⁶ or scaling-based¹¹⁷⁻¹¹⁹ modeling techniques. These traditional modeling techniques require accurate estimation of relevant properties to predict with high certainty, which is seldom the case^{114, 117}. Also, experiments are generally performed in a controlled environment with nearly ideal conditions, and modeling based on conventional techniques requires considerable data to be generated to check the effect of each parameter interaction. It is also challenging to account for the simultaneous interaction of various properties for predictive modeling for changing environments. In these scenarios, AI and ML approaches have been widely applied due to their ability to solve complicated problems¹²⁰. The modeling techniques like artificial neural network (ANN)¹²¹, Bayesian belief network (BBN)¹²² etc., are easily applicable in cases where the cause-effect relationship between the parameters possesses conceptual uncertainty. Training AI and ML-based methods may not require accurate asphaltene properties estimation and can predict the asphaltene deposition behavior in multiple scenarios. In an attempt to apply artificial intelligence for the prediction of asphaltene precipitation behaviour based on different variables, the authors used the BBN model¹²². It was found that the BBN model predicted the asphaltene precipitation with more confidence compared to other models and also covered the wide range of variables. Very recently, the three efficient artificial intelligent models, including group method of data handling (GMDH), least squares support vector machine (LSSVM), and artificial neural network (ANN), were proposed for estimating asphaltene adsorption on different nanocomposites based on only 252 data points¹²¹. The temperature was found to be most prominent parameter for asphaltene adsorption for model oil solutions. Literature reports other predictive modeling using Artificial Intelligence, which can

significantly reduce the experimental efforts and aid in modeling asphaltene precipitation approaches with greater confidence^{123, 124}. These simple methods showing the applicability of AI and ML with limited data when supplemented with microfluidics for high quality, rapid data generation capacity can result in new insights that have never been observed before.

5. INSIGHTS INTO THE ASPHALTENE DEPOSITION DYNAMICS AND OIL AND WATER EMULSION STABILIZATION VIA MICROFLUIDICS STUDIES

The scope of microfluidics is only limited to the way experiments are designed and the instruments available for characterization and generation of valuable data. Innovation in microfluidics and attached instrumentation has helped generate a lot of useful information and understanding of asphaltene deposition kinetics, the effect of oil well properties, and the role of asphaltene in oil-water emulsion stabilization. Studies in terms of understanding the role of demulsifiers and the additives in oil and water separation are designed to evaluate the efficacy between the different additives, which can help develop the suitable demulsifier as an asphaltene deposition mitigation technique. A good pore-scale understanding is necessary to solve the problem of asphaltene deposition in the reservoir, which has become feasible by microfluidics. The ability to mimic similar reservoir properties, generation of stable droplets and visual monitoring of coalescence, real-time measurement of chemical interaction, and change in chemical composition during asphaltene deposition have helped get deep insights about asphaltene, which is discussed in this section.

Steam solvent coinjection helps in improving the steam-assisted gravity drainage performance; however, it complicates the thermal process further by the addition of solvent. Steam saturation

temperature, degree of dilution (solvent-bitumen), steam solvent azeotropic temperature and asphaltene precipitation in condensing zone are important criteria on which performance depends. In contrast with pure solvents and condensate, naphtha results in the highest recovery due to a higher steam-solvent azeotropic temperature, effective dilution, with minimal asphaltene deposition⁷¹. As naphtha contains heavier hydrocarbon fraction and aromatic/naphthenic components, this helps reduce the deposition in larger pore sizes since the mobility of asphaltene decreases and cannot reach the nearest posts to block the entire path of the flow¹²⁵. The addition of solvent results in a non-equilibrium condition, and the local concentration of flocculants increase the threshold limit for asphaltene deposition. Solvents with higher diffusivity result in firm deposits fixed on the surface, whereas deposits can be easily taken from the channel in case of slow diffusion. Asphaltenes of different types and different hydrocarbon ratio starts to precipitate in the direction of solvent flow however, there is spatial inhomogeneity of precipitated asphaltene due to the varied composition and different functional groups⁶. Lighter solvents, e.g., n-pentane, tend to faster asphaltene precipitation with higher agglomeration and asphaltene deposition⁴⁷.

At solvent composition > 80% low molecular weight, asphaltenes are susceptible to be precipitated but are easier to dissolve, whereas higher temperature increases the asphaltene removal efficacy⁴⁶. It was observed that commercially used alkylphenol model chemical dispersants worsen the asphaltene deposition but the mechanism of permeability reduction and plugging in pores medium varies. As the deposition tendency is related to the intermolecular interactions governing the asphaltene dispersant system, injecting chemical dispersant reduces the size of asphaltene aggregates which results in a higher initial deposition rate; however, strong repulsive interactions make aggregates soft which can be easily eroded in shear flow after

deposition which in turn reduces the overall deposition rate⁹¹. Different microemulsions and equivalent surfactant packages can remove the asphaltene deposits. The removal efficiency depends on the solvent type in the microemulsion and their concentration. At low concentrations, the D-limonene-based microemulsion exhibits the best performance compared to the xylene-based microemulsion. The asphaltene-based micro-emulsion solubilizes the asphaltene deposits better in high and low permeability regions⁹³. Asphaltene molecules with larger sheet sizes are easier to dissolve in xylenes than smaller sheet sizes, and adding the acidity to the pores asphaltene dissolution percentage can be increased⁸⁵. It was also found that asphaltene deposited at higher temperatures is difficult to dissolve using xylene than deposited at lower temperature⁸⁶. Using xylenes for dissolution of asphaltene at low deposition temperature, xylene fluid path was mainly restricted by the pore size limitation, whereas at higher temperatures, alteration of surface chemistry was found to be dominant⁸⁶. The asphaltene deposition rate remains consistent with the deposition amount, and the pore-scale morphology changes even at similar deposition rates⁴⁸. In a separate study using the toluene as a solvent, it was found that having an emulsion helps in reducing the solvent requirement for the same deposition removal efficiency. 70-30 water in oil emulsion produced better results than other emulsions with more sweep efficiency¹²⁶.

$\text{Al}_2\text{O}_3/\text{SiO}_2$ ratio, an important characteristic of reservoir mineralogy, can significantly affect the asphaltene precipitation dynamics. The $\text{Al}_2\text{O}_3/\text{SiO}_2$ ratio of 1/16 leads to >10% higher bed occupancy and ~13% higher asphaltene sheet size when compared to a bed with no Al_2O_3 particles. Al_2O_3 works as a preventive agent by reducing the early pore throat plugging, which entraps more asphaltene, increasing the deposited sheet size and lowering the channeling¹⁷. Al_2O_3 attracts the asphaltene molecules with larger sheet sizes, which tend to self-assemble, forming hydrodynamic bridging within the porous media⁸⁵. Higher fractal dimension with larger

aggregates asphaltene can form at higher temperatures in a short period of time⁸⁶. Lower than expected pore throat permeability impairments have been characterized even after removing 70-90 wt.% asphaltene while remaining asphaltene plugs the pore throat of porous media, which restricts the flow⁴⁶. Real-time monitoring of asphaltene deposition resulted in different pore throat plugging behavior during different stages of deposition. During middle stage, asphaltene deposition increases by 3.8% compared to only 1.8% during late stage. In the middle stage snowball effect dominates by accelerating the plugging by reducing the width of pore throat or it blocks the current flow path and divert it to the new path.. However, decrease of detour paths reduced the snow-ball effect at the late stage, which was further confirmed with the reduction of the coordination number of pores⁹⁰. The concentration of precipitants directly affects the asphaltene precipitation dynamics, increasing the asphaltene deposits at higher concentrations with wider size distribution for a longer duration. Higher precipitant concentration can act counterintuitively, decreasing the number of deposits though it can increase the deposition rate.. The asphaltene deposition process is credited to the competition between the shear rate and deposition kinetics where higher flow rate displays the higher deposition kinetics. At higher deposition rate size of asphaltene deposits increase but number of deposits decrease. In the capillary flow experiments it was observed that asphaltene deposition depends on the adsorption force where hydrodynamic effects and shear removal are less significant⁸². At the pore throat matrix which are perpendicular to the flow direction hinders the flow resulting in the faster deposition (fouling) around pore throat over precipitation. Hydrophilicity of the surface increases the deposition because at higher hydrophobicity surface energy is low and asphaltene molecules have less surface to attached to form deposits⁴⁷.

The separation of water from crude oil is also a necessary process. Understanding the asphaltene precipitation helps avoid the condition favorable for precipitation during extraction and transportation, which can help in easily feasible separation. In addition, monitoring the oil-water interface and the droplet coalescence in the presence of other chemical additives and demulsifiers is also of significant interest to the scientific community. By observing the interface and measuring the coalescence rate of droplets, it is possible to get the efficacy of the additive and demulsifier, which can help in rapid screening of the suitable choice through microfluidics. Coalescence probability is a reasonable indicator of the efficiency of the chosen demulsifier and the concentration at which it can be added to the crude oil. This coalescence probability can be easily calculated by observing the change in the droplet size over the flow path through optical visualization techniques and the coalescence rate can be calculated⁹⁶. Asphaltene tends to stabilize the oil-water emulsion, which creates difficulties separating water from the crude oil, especially when water is injected into the reservoir. The interfacial shear viscosity of asphaltene and water is strongest compared to other SARA components, resulting in the strongest strength of the interfacial film, which creates difficulty in the coalescence of water molecules, making separation cumbersome¹²⁷.

Asphaltene to absorbed on the surface of inorganic particles, the accumulation of these particles at the interface increases the interfacial tension. Stabilization of emulsion can adversely affect the oil separation and production where combination of asphaltene concentration, temperature of operation, concentration of inorganic particles and aging time are some of the important parameters to consider⁸⁴. In a study to choose between the two different additives, the coalescence frequency was measured on microfluidics, which was higher for one of the additives. At lower concentrations, it was seen that the demulsifier becomes diffusion-limited to

the interface, which allows the formation of droplet-stabilizing film and reduces the performance. Additive alters the interface, which aids in coalescence, whereas its ability to absorb to the interface rapidly is determinant of the performance. However, What makes one additive more effective than the other in preventing elastic film formation remains unclear⁹⁷. Recently, it was experimentally shown that chemical demulsifiers act on a limited timescale and specifically impact the soft regions in asphaltene film . These effects were observed for the ethylcellulose as demulsifier, which slows down the asphaltene deposition, disrupts interfacial structure formation, and forms the soft interfacial layers compared with asphaltene alone¹²⁸. A novel aliphatic alcohol nonionic polyether demulsifier was synthesized in a recent study, containing oxygen groups, e.g., hydroxyl, ester groups, carboxyl groups, ether groups, etc. This demulsifier breaks the interfacially active asphaltene films at the oil-water interface, which is then replaced by hydrogen bonding; however, the process strongly depends on the demulsifier concentration, temperature, and settling time which is also true for the other demulsifier studied in the literature¹²⁹.

Attachment of crude oil droplets with gas bubbles through the spreading mechanism was monitored via microfluidics. It was found that attachment efficiency increases at low or neutral pH. Reduction in salinity increases the electrostatic repulsion, whereas dissolved components stabilize the oil drops and gas bubbles, negatively impacting the attachment. Having small drops and a lower concentration of oil drops is beneficial for improving attachment efficiency⁹⁸. The crude oil and water phase composition influences coalescence time and droplet size distribution after the droplet merging. Coalescence is always most extensive with the shortest aged droplets, and larger droplet size distribution reduces the coalescence; however, these effects are oil

specific⁹⁹. Molecular symmetry and the presence of interfacially active groups are also essential factors to consider when choosing the effective demulsifier⁹².

Temperature and pressure in the reservoir also play a critical role in enhanced oil recovery processes, resulting in destabilization of the emulsion. Water droplets in oil coalesce at higher temperatures, destabilizing the emulsion, which can be separated easily. An increase in pressure helps in emulsion stabilization, reaching a plateau (optimum), after which pressure increment results in destabilization of the emulsion, which can be characterized by the amount of asphaltene precipitation. It was seen that at pressure up to 27579 kPa presence of asphaltene stabilized the emulsion; however, beyond that though the solubility of asphaltene increased emulsion stability decreased¹³⁰.

6. CHALLENGES AND PERSPECTIVE

Microfluidics has helped advance the knowledge about asphaltene deposition dynamics relevant to the reservoir rock porous structures and testing different inhibitors for prohibiting deposition. However, the microfluidics experiments mainly were in an ideal environment compared to the high pressure and high-temperature conditions that prevailed in the deep-sea environment. High-pressure microfluidics create the possibility of studying asphaltenes with live conditions, though cost and safety considerations remain challenges. The 2D porous structure fabricated in microfluidics is, for the most part, in geometrical symmetry, which is not the case in the reservoir or rock pores. Advancements in the design of porous media in microfluidics could lead to field scale pore physics. The chemical and surface properties in the reservoir rocks are far from ideal, which is critical for mimicking the exact physical environment. Incorporating the

chemical and surface similarity in the microporous structure in the microchannel is a significant challenge in simulating reservoir conditions. Most of the studies in microfluidics are performed in isolation at regulated flow rates with uniform flow profiles, which help understand the complicated dynamics but are challenging to replicate in the field where radial flow from the wellbore is typical. Also, as crude oil and reservoir properties vary based on location, no approaches have been developed to generalize results obtained in the microfluidic devices. As conditions in microfluidics experimentations are well controlled, any change in the specific properties may drastically impact the results obtained.

Reservoir rocks are made up of nanoscale chemical and physical characteristics, and it is challenging to fabricate nanoporous structures in microfluidics and to incorporate visualization techniques for the observation at the nanoscale. There have been signs of progress in visualizing interfaces for oil and water coalescence, but the effective methodology to study the kinetics of interaction between phases is not well established. All microfluidics produce reproducible results but depend on the reproducibility of the parameters and composition of the materials used. Applied methods are ideal, and data generated will require appropriate kinetics models before field application. Nanoaggregation models developed for asphaltenes could lead to deeper understanding of their physical structure in porous media, towards a more comprehensive experimental approach. Related to that point, the development of advanced in situ analytical methods, such as small angle or neutron scattering could generate a wealth of data on the chemical and physical rate processes within the porous media. Reconstructing the porous media, both experimentally and computationally, in which synchronous discovery of asphaltenes mechanisms is performed could generate massive amounts of data, prompting big data analysis and the need for deep learning methods where computers work synchronous with microfluidics.

7. CONCLUSION

Asphaltenes remain a central problem in the flow assurance of energy that drives the global economy. Understanding and monitoring the asphaltene deposition processes and dynamics in the presence of different chemicals and additives in varying environments will help formulate the strategies for mitigating asphaltene deposition during extraction and transportation. Conventional methodologies of asphaltene analysis and related experimentations are cumbersome to utilize and are expensive in terms of time and energy. In the era of globalization and ever-expanding economies, fast, simple, reliable, and sustainable techniques to generate valuable knowledge that can quickly materialize becomes desirable. Microfluidics is an advanced synthesis and analysis tool that has proven its importance in the different areas of science and engineering as a cost-effective and sustainable way of development.

When integrated with powerful instruments that can probe the system's characteristics at significantly high resolution compared to the bulk analysis, Microfluidics can generate valuable information in a fraction of time. The ability to mimic the reservoir's porous nature and high-resolution imaging helps understand the asphaltene deposition, its interfacial properties, and possible mitigation solutions by studying the role of different solvents and additives.

Miniaturization also results in less volume consumption for experiments/analysis and shorter duration, which is an added advantage in cost reduction, sustainability, and fast measurement.

High throughput screening is possible only with microfluidics, which can be implemented at the point of use and can help rapid screening between the efficacy of different demulsifiers or solvents. Microfluidics experimentation makes real-time feedback with field operations a

possibility, and advanced data analytics algorithms developed in recent years could improve the efficiency of reservoir operations. Ultra-high pressure microfluidics, for deep water applications, prompting the development of new device fabrication methods with in situ analytics will likely supplement their utilization to a much greater extent to generate new insights in the years to come.

AUTHOR INFORMATION

Corresponding Author

Ryan L. Hartman - Department of Chemical and Biomolecular Engineering, NYU Tandon School of Engineering, Brooklyn, New York, 11201, United States.

Email: ryan.hartman@nyu.edu

Authors

Mrityunjay K. Sharma - Department of Chemical and Biomolecular Engineering, NYU Tandon School of Engineering, Brooklyn, New York, 11201, United States.

Email: mks9817@nyu.edu

Author Contributions

The manuscript was written through contributions of all authors. Conceptualization: R.L.H. Writing original draft: M.K.S.; Writing review & editing: M.K.S. and R.L.H. Corresponding: R.L.H. All authors have given approval to the final version of the manuscript.

ACKNOWLEDGMENT

This material is based upon work supported by the U.S. Department of Energy, Office of Science, Office of Basic Energy Sciences Synthesis and Processing Science program under Award Number DE-SC-0022161.

AUTHOR BIOGRAPHIES

Mrityunjay K. Sharma received his B.Tech from the Institute of Chemical Technology and Ph.D. from the National Chemical Laboratory, India. He is currently a Postdoctoral Associate at New York University in the Chemical and Biomolecular Engineering department. His research interests revolve around the use of continuous flow microreactors for reaction engineering, the study of gas hydrates, and the use of machine learning to scale up challenging pharmaceuticals chemistries.

Ryan L. Hartman is Associate Professor in Chemical and Biomolecular Engineering at New York University. He completed his BS at Michigan Technological University, Ph.D. at the University of Michigan, and postdoctoral training at the Massachusetts Institute of Technology, all in chemical engineering. He is a member of the National Academy of Inventors. His research interests revolve around the design of artificial intelligence with continuous-flow microreactors for the discovery of reaction kinetics and mechanisms.

REFERENCES

- (1) Goual, L. Petroleum asphaltenes. *Crude oil emulsions—composition stability and characterization*, ed. ME Abdul-Raouf **2012**, 27-42.
- (2) Kokal, S. L.; Sayegh, S. G. Asphaltenes: the cholesterol of petroleum. In *Middle East oil show*, 1995; OnePetro.
- (3) Pazuki, G. R.; Nikookar, M.; Omidkhah, M. R. Application of a new cubic equation of state to computation of phase behavior of fluids and asphaltene precipitation in crude oil. *Fluid Phase Equilibria* **2007**, 254 (1-2), 42-48.
- (4) Langevin, D.; Argillier, J.-F. Interfacial behavior of asphaltenes. *Advances in colloid and interface science* **2016**, 233, 83-93.
- (5) Sieben, V. J.; Tharanivasan, A. K.; Andersen, S. I.; Mostowfi, F. Microfluidic approach for evaluating the solubility of crude oil asphaltenes. *Energy & Fuels* **2016**, 30 (3), 1933-1946.
- (6) Shalygin, A. S.; Kozhevnikov, I. V.; Kazarian, S. G.; Martyanov, O. N. Spectroscopic imaging of deposition of asphaltenes from crude oil under flow. *Journal of Petroleum Science and Engineering* **2019**, 181, 106205.
- (7) Schneider, M. H.; Sieben, V. J.; Kharrat, A. M.; Mostowfi, F. Measurement of asphaltenes using optical spectroscopy on a microfluidic platform. *Analytical chemistry* **2013**, 85 (10), 5153-5160.
- (8) David Ting, P.; Hirasaki, G. J.; Chapman, W. G. Modeling of asphaltene phase behavior with the SAFT equation of state. *Petroleum Science and Technology* **2003**, 21 (3-4), 647-661.

- (9) Vargas, F. M.; Gonzalez, D. L.; Hirasaki, G. J.; Chapman, W. G. Modeling asphaltene phase behavior in crude oil systems using the perturbed chain form of the statistical associating fluid theory (PC-SAFT) equation of state. *Energy & Fuels* **2009**, *23* (3), 1140-1146.
- (10) Panuganti, S. R.; Vargas, F. M.; Gonzalez, D. L.; Kurup, A. S.; Chapman, W. G. PC-SAFT characterization of crude oils and modeling of asphaltene phase behavior. *Fuel* **2012**, *93*, 658-669.
- (11) Shirani, B.; Nikazar, M.; Mousavi-Dehghani, S. A. Prediction of asphaltene phase behavior in live oil with CPA equation of state. *Fuel* **2012**, *97*, 89-96.
- (12) Zhang, X.; Pedrosa, N.; Moorwood, T. Modeling asphaltene phase behavior: comparison of methods for flow assurance studies. *Energy & Fuels* **2012**, *26* (5), 2611-2620.
- (13) Wang, S.; Segin, N.; Wang, K.; Masliyah, J. H.; Xu, Z. Wettability control mechanism of highly contaminated hydrophilic silica/alumina surfaces by ethyl cellulose. *The Journal of Physical Chemistry C* **2011**, *115* (21), 10576-10587.
- (14) Alboudwarej, H.; Pole, D.; Svrcek, W. Y.; Yarranton, H. W. Adsorption of asphaltenes on metals. *Industrial & engineering chemistry research* **2005**, *44* (15), 5585-5592.
- (15) Ortega-Rodriguez, A.; Cruz, S.; Garcia-Cruz, I.; Lira-Galeana, C. Study of the adhesion force of asphaltene aggregates to metallic surfaces of Fe and Al. *Energy & Fuels* **2016**, *30* (5), 3596-3604.
- (16) Mohammadi, M.; Akbari, M.; Fakhroueian, Z.; Bahramian, A.; Azin, R.; Arya, S. Inhibition of asphaltene precipitation by TiO₂, SiO₂, and ZrO₂ nanofluids. *Energy & Fuels* **2011**, *25* (7), 3150-3156.

- (17) Pinho, B.; Minsariya, K.; Yen, A.; Joshi, N.; Hartman, R. L. Role of HZSM-5 Aluminosilicates on Asphaltenes Deposition by High-Throughput in Situ Characterizations of a Microreservoir. *Energy & Fuels* **2017**, *31* (11), 11640-11650.
- (18) Mullins, O. C.; Sheu, E. Y.; Hammami, A.; Marshall, A. G. *Asphaltenes, heavy oils, and petroleomics*; Springer Science & Business Media, 2007.
- (19) Enayat, S.; Tavakkoli, M.; Yen, A.; Misra, S.; Vargas, F. M. Review of the current laboratory methods to select asphaltene inhibitors. *Energy & Fuels* **2020**, *34* (12), 15488-15501.
- (20) Karambeigi, M. A.; Nikazar, M.; Kharrat, R. Experimental evaluation of asphaltene inhibitors selection for standard and reservoir conditions. *Journal of Petroleum Science and Engineering* **2016**, *137*, 74-86.
- (21) Bahman, J.; Sharifi, K.; Nasiri, M.; Asl, M. H. Development of a Log-Log scaling law approach for prediction of asphaltene precipitation from crude oil by n-alkane titration. *Journal of Petroleum Science and Engineering* **2018**, *160*, 393-400.
- (22) Melendez-Alvarez, A. A.; Garcia-Bermudes, M.; Tavakkoli, M.; Doherty, R. H.; Meng, S.; Abdallah, D. S.; Vargas, F. M. On the evaluation of the performance of asphaltene dispersants. *Fuel* **2016**, *179*, 210-220.
- (23) Atta, A. M.; Ezzat, A. O.; Abdullah, M. M.; Hashem, A. I. Effect of different families of hydrophobic anions of imadazolium ionic liquids on asphaltene dispersants in heavy crude oil. *Energy & Fuels* **2017**, *31* (8), 8045-8053.

- (24) Wang, X.; Zhang, H.; Liang, X.; Shi, L.; Chen, M.; Wang, X.; Liu, W.; Ye, Z. New amphiphilic macromolecule as viscosity reducer with both asphaltene dispersion and emulsifying capacity for offshore heavy oil. *Energy & Fuels* **2021**, *35* (2), 1143-1151.
- (25) Palermo, L. C.; Lucas, E. F. Asphaltene aggregation: influence of composition of copolymers based on styrene-stearyl methacrylate and styrene-stearyl cinnamate containing sulfate groups. *Energy & Fuels* **2016**, *30* (5), 3941-3946.
- (26) Liu, G.; Yang, J.; Song, J.; Xu, X. Inhibition of asphaltene precipitation in blended crude oil using novel oil-soluble maleimide polymers. *Energy Sources, Part A: Recovery, Utilization, and Environmental Effects* **2019**, *41* (20), 2460-2470.
- (27) Firoozinia, H.; Fouladi Hossein Abad, K.; Varamesh, A. A comprehensive experimental evaluation of asphaltene dispersants for injection under reservoir conditions. *Petroleum Science* **2016**, *13* (2), 280-291.
- (28) Li, X.; Lu, S.; Niu, M.; Cheng, R.; Gong, Y.; Xu, J. Asphaltene Inhibition and Flow Improvement of Crude Oil with a High Content of Asphaltene and Wax by Polymers Bearing Ultra-Long Side Chain. *Energies* **2021**, *14* (24), 8243.
- (29) Kharrat, A. M.; Indo, K.; Mostowfi, F. Asphaltene content measurement using an optical spectroscopy technique. *Energy & Fuels* **2013**, *27* (5), 2452-2457.
- (30) Li, X.; Chi, P.; Guo, X.; Sun, Q. Effects of asphaltene concentration and asphaltene agglomeration on viscosity. *Fuel* **2019**, *255*, 115825.
- (31) Rogel, E.; Ovalles, C.; Vien, J.; Moir, M. Asphaltene content by the in-line filtration method. *Fuel* **2016**, *171*, 203-209.

- (32) Fotland, P.; Anfindsen, H.; Fadnes, F. H. Detection of asphaltene precipitation and amounts precipitated by measurement of electrical conductivity. *Fluid Phase Equilibria* **1993**, *82*, 157-164.
- (33) Eyssautier, J.; Frot, D.; Barré, L. Structure and dynamic properties of colloidal asphaltene aggregates. *Langmuir* **2012**, *28* (33), 11997-12004.
- (34) Daridon, J.-L.; Carrier, H. Measurement of phase changes in live crude oil using an acoustic wave sensor: Asphaltene instability envelope. *Energy & Fuels* **2017**, *31* (9), 9255-9267.
- (35) Buckley, J. S. Predicting the onset of asphaltene precipitation from refractive index measurements. *Energy & Fuels* **1999**, *13* (2), 328-332.
- (36) Lashkarbolooki, M.; Ayatollahi, S. Effects of asphaltene, resin and crude oil type on the interfacial tension of crude oil/brine solution. *Fuel* **2018**, *223*, 261-267.
- (37) Clarke, P. F.; Pruden, B. B. Asphaltene precipitation: detection using heat transfer analysis, and inhibition using chemical additives. *Fuel* **1997**, *76* (7), 607-614.
- (38) Guzmán, R.; Ancheyta, J.; Trejo, F.; Rodríguez, S. Methods for determining asphaltene stability in crude oils. *Fuel* **2017**, *188*, 530-543.
- (39) Wang, S.; Chen, S.; Li, Z. Characterization of produced and residual oils in the CO₂ flooding process. *Energy & Fuels* **2016**, *30* (1), 54-62.
- (40) Fakher, S.; Imqam, A.; Wanas, E. Investigating the viscosity reduction of ultra-heavy crude oil using hydrocarbon soluble low molecular weight compounds to improve oil production and transportation. In *SPE International Heavy Oil Conference and Exhibition*, 2018; OnePetro.

- (41) Mozaffari, S.; Ghasemi, H.; Tchoukov, P.; Czarnecki, J.; Nazemifard, N. Lab-on-a-chip systems in asphaltene characterization: a review of recent advances. *Energy & Fuels* **2021**, *35* (11), 9080-9101.
- (42) Elvira, K. S.; Wootton, R. C.; deMello, A. J. The past, present and potential for microfluidic reactor technology in chemical synthesis. *Nature chemistry* **2013**, *5* (11), 905-915.
- (43) Scheler, O.; Postek, W.; Garstecki, P. Recent developments of microfluidics as a tool for biotechnology and microbiology. *Current opinion in biotechnology* **2019**, *55*, 60-67.
- (44) Pandey, C. M.; Augustine, S.; Kumar, S.; Kumar, S.; Nara, S.; Srivastava, S.; Malhotra, B. D. Microfluidics based point-of-care diagnostics. *Biotechnology journal* **2018**, *13* (1), 1700047.
- (45) Niculescu, A.-G.; Chircov, C.; Bîrcă, A. C.; Grumezescu, A. M. Nanomaterials synthesis through microfluidic methods: An updated overview. *Nanomaterials* **2021**, *11* (4), 864.
- (46) Hu, C.; Yen, A.; Joshi, N.; Hartman, R. L. Packed-bed microreactors for understanding of the dissolution kinetics and mechanisms of asphaltenes in xylenes. *Chemical Engineering Science* **2016**, *140*, 144-152.
- (47) Keshmiri, K.; Huang, H.; Nazemifard, N. Microfluidic platform to evaluate asphaltene deposition during solvent-based extraction of bitumen. *Fuel* **2019**, *239*, 841-851.
- (48) Lin, Y.-J.; Cao, T.; Chacón-Patiño, M. L.; Rowland, S. M.; Rodgers, R. P.; Yen, A.; Biswal, S. L. Microfluidic study of the deposition dynamics of asphaltene subfractions enriched with island and archipelago motifs. *Energy & Fuels* **2019**, *33* (3), 1882-1891.

- (49) Pagán Pagán, N. M.; Zhang, Z.; Nguyen, T. V.; Marciel, A. B.; Biswal, S. L. Physicochemical Characterization of Asphaltenes Using Microfluidic Analysis. *Chemical Reviews* **2022**.
- (50) Chen, Q.; Li, G.; Jin, Q.-H.; Zhao, J.-L.; Ren, Q.-S.; Xu, Y.-S. A rapid and low-cost procedure for fabrication of glass microfluidic devices. *Journal of microelectromechanical systems* **2007**, *16* (5), 1193-1200.
- (51) Iliescu, C.; Taylor, H.; Avram, M.; Miao, J.; Franssila, S. A practical guide for the fabrication of microfluidic devices using glass and silicon. *Biomicrofluidics* **2012**, *6* (1), 016505.
- (52) Stjernström, M.; Roeraade, J. Method for fabrication of microfluidic systems in glass. *Journal of Micromechanics and Microengineering* **1998**, *8* (1), 33.
- (53) Hwang, J.; Cho, Y. H.; Park, M. S.; Kim, B. H. Microchannel fabrication on glass materials for microfluidic devices. *International Journal of Precision Engineering and Manufacturing* **2019**, *20* (3), 479-495.
- (54) Jia, Z.-J.; Fang, Q.; Fang, Z.-L. Bonding of glass microfluidic chips at room temperatures. *Analytical chemistry* **2004**, *76* (18), 5597-5602.
- (55) Lin, C.-H.; Lee, G.-B.; Lin, Y.-H.; Chang, G.-L. A fast prototyping process for fabrication of microfluidic systems on soda-lime glass. *Journal of Micromechanics and Microengineering* **2001**, *11* (6), 726.
- (56) Leester-Schädel, M.; Lorenz, T.; Jürgens, F.; Richter, C. Fabrication of microfluidic devices. In *Microsystems for Pharmatechnology*, Springer, 2016; pp 23-57.

- (57) Harris, N.; Hill, M.; Beeby, S.; Shen, Y.; White, N.; Hawkes, J.; Coakley, W. A silicon microfluidic ultrasonic separator. *Sensors and Actuators B: Chemical* **2003**, *95* (1-3), 425-434.
- (58) Becker, H.; Locascio, L. E. Polymer microfluidic devices. *Talanta* **2002**, *56* (2), 267-287.
- (59) McDonald, J. C.; Duffy, D. C.; Anderson, J. R.; Chiu, D. T.; Wu, H.; Schueller, O. J.; Whitesides, G. M. Fabrication of microfluidic systems in poly (dimethylsiloxane). *ELECTROPHORESIS: An International Journal* **2000**, *21* (1), 27-40.
- (60) Tan, W.; Desai, T. A. Layer-by-layer microfluidics for biomimetic three-dimensional structures. *Biomaterials* **2004**, *25* (7-8), 1355-1364.
- (61) Plecis, A.; Chen, Y. Fabrication of microfluidic devices based on glass–PDMS–glass technology. *Microelectronic engineering* **2007**, *84* (5-8), 1265-1269.
- (62) Barker, S. L.; Tarlov, M. J.; Canavan, H.; Hickman, J. J.; Locascio, L. E. Plastic microfluidic devices modified with polyelectrolyte multilayers. *Analytical Chemistry* **2000**, *72* (20), 4899-4903.
- (63) Nishat, S.; Jafry, A. T.; Martinez, A. W.; Awan, F. R. based microfluidics: Simplified fabrication and assay methods. *Sensors and Actuators B: Chemical* **2021**, *336*, 129681.
- (64) Brandner, J. J. Fabrication of microreactors made from metals and ceramics. *Microreactors in Organic Synthesis and Catalysis* **2008**, 1-17.
- (65) Wan, Y. S. S.; Chau, J. L. H.; Gavriilidis, A.; Yeung, K. L. Design and fabrication of zeolite-based microreactors and membrane microseparators. *Microporous and Mesoporous Materials* **2001**, *42* (2-3), 157-175.

- (66) Kim, M.; Sell, A.; Sinton, D. Aquifer-on-a-Chip: understanding pore-scale salt precipitation dynamics during CO₂ sequestration. *Lab on a Chip* **2013**, *13* (13), 2508-2518.
- (67) Conn, C. A.; Ma, K.; Hirasaki, G. J.; Biswal, S. L. Visualizing oil displacement with foam in a microfluidic device with permeability contrast. *Lab on a Chip* **2014**, *14* (20), 3968-3977.
- (68) Hu, C.; Morris, J. E.; Hartman, R. L. Microfluidic investigation of the deposition of asphaltenes in porous media. *Lab on a Chip* **2014**, *14* (12).
- (69) Kord, S.; Miri, R.; Ayatollahi, S.; Escrochi, M. Asphaltene deposition in carbonate rocks: experimental investigation and numerical simulation. *Energy & Fuels* **2012**, *26* (10), 6186-6199.
- (70) Davudov, D.; Moghanloo, R. G. A new model for permeability impairment due to asphaltene deposition. *Fuel* **2019**, *235*, 239-248.
- (71) Xu, L.; Abedini, A.; Qi, Z.; Kim, M.; Guerrero, A.; Sinton, D. Pore-scale analysis of steam-solvent coinjection: azeotropic temperature, dilution and asphaltene deposition. *Fuel* **2018**, *220*, 151-158.
- (72) Dindoruk, B.; Ratnakar, R. R.; He, J. Review of recent advances in petroleum fluid properties and their representation. *Journal of Natural Gas Science and Engineering* **2020**, *83*, 103541.
- (73) Otumudia, E.; Hamidi, H.; Jadhawar, P.; Wu, K. Effects of reservoir rock pore geometries and ultrasonic parameters on the removal of asphaltene deposition under ultrasonic waves. *Ultrasonics sonochemistry* **2022**, *83*, 105949.

(74) Fakher, S.; Ahdaya, M.; Elturki, M.; Imqam, A. Critical review of asphaltene properties and factors impacting its stability in crude oil. *Journal of Petroleum Exploration and Production Technology* **2020**, *10* (3), 1183-1200.

(75) Schuler, B.; Zhang, Y.; Liu, F.; Pomerantz, A. E.; Andrews, A. B.; Gross, L.; Pauchard, V.; Banerjee, S.; Mullins, O. C. Overview of asphaltene nanostructures and thermodynamic applications. *Energy & Fuels* **2020**, *34* (12), 15082-15105.

(76) Mullins, O. C. The asphaltenes. *Annual review of analytical chemistry* **2011**, *4*, 393-418.

(77) Bojang, A. A.; Wu, H.-S. Design, fundamental principles of fabrication and applications of microreactors. *Processes* **2020**, *8* (8), 891.

(78) Ren, K.; Zhou, J.; Wu, H. Materials for microfluidic chip fabrication. *Accounts of chemical research* **2013**, *46* (11), 2396-2406.

(79) Bowden, S. A.; Monaghan, P.; Wilson, R.; Parnell, J.; Cooper, J. The liquid-liquid diffusive extraction of hydrocarbons from a North Sea oil using a microfluidic format. *Lab on a Chip* **2006**, *6* (6), 740-743.

(80) Bowden, S. A.; Wilson, R.; Parnell, J.; Cooper, J. M. Determination of the asphaltene and carboxylic acid content of a heavy oil using a microfluidic device. *Lab on a Chip* **2009**, *9* (6), 828-832.

(81) Alabi, O. O.; Bowden, S. A.; Parnell, J. Simultaneous and rapid asphaltene and TAN determination for heavy petroleum using an H-cell. *Analytical Methods* **2014**, *6* (11), 3651-3660.

(82) Li, X.; Guo, Y.; Sun, Q.; Lan, W.; Liu, A.; Guo, X. Experimental study for the impacts of flow rate and concentration of asphaltene precipitant on dynamic asphaltene deposition in microcapillary medium. *Journal of Petroleum Science and Engineering* **2018**, *162*, 333-340.

(83) Meng, J.; You, J. B.; Arends, G. F.; Hao, H.; Tan, X.; Zhang, X. Microfluidic device coupled with total internal reflection microscopy for in situ observation of precipitation. *The European Physical Journal E* **2021**, *44* (4), 1-8.

(84) Hu, C.; Garcia, N. C.; Xu, R.; Cao, T.; Yen, A.; Garner, S. A.; Macias, J. M.; Joshi, N.; Hartman, R. L. Interfacial properties of asphaltenes at the heptol–brine interface. *Energy & Fuels* **2016**, *30* (1), 80-87.

(85) Chen, W.; Vashistha, P.; Yen, A.; Joshi, N.; Kapoor, Y.; Hartman, R. L. Asphaltenes dissolution mechanism study by in situ Raman characterization of a packed-bed microreactor with HZSM-5 Aluminosilicates. *Energy & Fuels* **2018**, *32* (12), 12205-12217.

(86) Chen, W.; Guo, T.; Kapoor, Y.; Russell, C.; Juyal, P.; Yen, A.; Hartman, R. L. An automated microfluidic system for the investigation of asphaltene deposition and dissolution in porous media. *Lab on a Chip* **2019**, *19* (21), 3628-3640.

(87) Leary, T.; Yeganeh, M.; Maldarelli, C. Microfluidic study of the electrocoalescence of aqueous droplets in crude oil. *ACS omega* **2020**, *5* (13), 7348-7360.

(88) Morin, B.; Liu, Y.; Alvarado, V.; Oakey, J. A microfluidic flow focusing platform to screen the evolution of crude oil–brine interfacial elasticity. *Lab on a Chip* **2016**, *16* (16), 3074-3081.

(89) Liu, Y.; Kaszuba, J.; Oakey, J. Microfluidic investigations of crude oil-brine interface elasticity modifications via brine chemistry to enhance oil recovery. *Fuel* **2019**, *239*, 338-346.

(90) Onaka, Y.; Sato, K. Dynamics of pore-throat plugging and snow-ball effect by asphaltene deposition in porous media micromodels. *Journal of Petroleum Science and Engineering* **2021**, *207*, 109176.

(91) Lin, Y.-J.; He, P.; Tavakkoli, M.; Mathew, N. T.; Fatt, Y. Y.; Chai, J. C.; Goharzadeh, A.; Vargas, F. M.; Biswal, S. L. Characterizing asphaltene deposition in the presence of chemical dispersants in porous media micromodels. *Energy & Fuels* **2017**, *31* (11), 11660-11668.

(92) Zhang, Z.; Song, J.; Lin, Y.-J.; Wang, X.; Biswal, S. L. Comparing the coalescence rate of water-in-oil emulsions stabilized with asphaltenes and asphaltene-like molecules. *Langmuir* **2020**, *36* (27), 7894-7900.

(93) Zhang, Z.; Perrard, A.; Trabelsi, S.; Biswal, S. L. Evaluation of Asphaltene Remediation Using Microemulsion Formulations in a Porous Media Microfluidic Device. *Energy & Fuels* **2021**, *35* (14), 11162-11170.

(94) Kataoka, E. M.; Murer, R. C.; Santos, J. M.; Carvalho, R. M.; Eberlin, M. N.; Augusto, F.; Poppi, R. J.; Gobbi, A. L.; Hantao, L. W. Simple, expendable, 3D-printed microfluidic systems for sample preparation of petroleum. *Analytical chemistry* **2017**, *89* (6), 3460-3467.

(95) Nielsen, J. B.; Hanson, R. L.; Almughamsi, H. M.; Pang, C.; Fish, T. R.; Woolley, A. T. Microfluidics: innovations in materials and their fabrication and functionalization. *Analytical chemistry* **2019**, *92* (1), 150-168.

(96) Tian, Y. S.; Yang, Z. Q.; Thoroddsen, S. T.; Elsaadawy, E. A new image-based microfluidic method to test demulsifier enhancement of coalescence-rate, for water droplets in crude oil. *Journal of Petroleum Science and Engineering* **2022**, *208*, 109720.

- (97) Nowbahar, A.; Whitaker, K. A.; Schmitt, A. K.; Kuo, T.-C. Mechanistic study of water droplet coalescence and flocculation in diluted bitumen emulsions with additives using microfluidics. *Energy & Fuels* **2017**, *31* (10), 10555-10565.
- (98) Dudek, M.; Øye, G. Microfluidic study on the attachment of crude oil droplets to gas bubbles. *Energy & Fuels* **2018**, *32* (10), 10513-10521.
- (99) Dudek, M.; Chicault, J.; Øye, G. Microfluidic investigation of crude oil droplet coalescence: effect of oil/water composition and droplet aging. *Energy & Fuels* **2019**, *34* (5), 5110-5120.
- (100) Kole, S.; Bikkina, P. A parametric study on the application of microfluidics for emulsion characterization. *Journal of Petroleum Science and Engineering* **2017**, *158*, 152-159.
- (101) Talebi, S.; Abedini, A.; Lele, P.; Guerrero, A.; Sinton, D. Microfluidics-based measurement of solubility and diffusion coefficient of propane in bitumen. *Fuel* **2017**, *210*, 23-31.
- (102) Lisitza, N. V.; Freed, D. E.; Sen, P. N.; Song, Y.-Q. Study of asphaltene nanoaggregation by nuclear magnetic resonance (NMR). *Energy & Fuels* **2009**, *23* (3), 1189-1193.
- (103) Fergoug, T.; Bouhadda, Y. Determination of Hassi Messaoud asphaltene aromatic structure from ¹H & ¹³C NMR analysis. *Fuel* **2014**, *115*, 521-526.
- (104) Ok, S.; Mal, T. K. NMR spectroscopy analysis of asphaltenes. *Energy & Fuels* **2019**, *33* (11), 10391-10414.
- (105) AlHumaidan, F. S.; Hauser, A.; Rana, M. S.; Lababidi, H. M. NMR characterization of asphaltene derived from residual oils and their thermal decomposition. *Energy & Fuels* **2017**, *31* (4), 3812-3820.

(106) Vukovic, J. P.; Novak, P.; Jednacak, T. NMR Spectroscopy as a Tool for Studying Asphaltene Composition. *Croatica Chemica Acta* **2019**, *92* (3), 1G-1G.

(107) Asemani, M.; Rabbani, A. R. Oil-oil correlation by FTIR spectroscopy of asphaltene samples. *Geosciences Journal* **2016**, *20* (2), 273-283.

(108) Gabrienko, A. A.; Morozov, E. V.; Subramani, V.; Martyanov, O. N.; Kazarian, S. G. Chemical visualization of asphaltenes aggregation processes studied in situ with ATR-FTIR spectroscopic imaging and NMR imaging. *The Journal of Physical Chemistry C* **2015**, *119* (5), 2646-2660.

(109) Taherian, Z.; Dehaghani, A. S.; Ayatollahi, S.; Kharrat, R. A new insight to the assessment of asphaltene characterization by using fourier transformed infrared spectroscopy. *Journal of Petroleum Science and Engineering* **2021**, *205*, 108824.

(110) Meng, J.; You, J. B.; Hao, H.; Tan, X.; Zhang, X. Primary submicron particles from early stage asphaltene precipitation revealed in situ by total internal reflection fluorescence microscopy in a model oil system. *Fuel* **2021**, *296*, 120584.

(111) Goncalves, S.; Castillo, J.; Fernandez, A.; Hung, J. Absorbance and fluorescence spectroscopy on the aggregation behavior of asphaltene–toluene solutions. *Fuel* **2004**, *83* (13), 1823-1828.

(112) Hung, A. M.; Fini, E. H. Absorption spectroscopy to determine the extent and mechanisms of aging in bitumen and asphaltenes. *Fuel* **2019**, *242*, 408-415.

- (113) Evdokimov, I. N.; Eliseev, N. Y.; Akhmetov, B. Assembly of asphaltene molecular aggregates as studied by near-UV/visible spectroscopy: I. Structure of the absorbance spectrum. *Journal of Petroleum Science and Engineering* **2003**, *37* (3-4), 135-143.
- (114) Andersen, S. I.; Speight, J. G. Thermodynamic models for asphaltene solubility and precipitation. *Journal of Petroleum Science and Engineering* **1999**, *22* (1-3), 53-66.
- (115) Subramanian, S.; Simon, S.; Sjöblom, J. Asphaltene precipitation models: a review. *Journal of Dispersion Science and Technology* **2016**, *37* (7), 1027-1049.
- (116) Daryasafar, A.; Masoudi, M.; Kord, S.; Madani, M. Evaluation of different thermodynamic models in predicting asphaltene precipitation: A comparative study. *Fluid Phase Equilibria* **2020**, *514*, 112557.
- (117) Ashoori, S.; Abedini, A.; Abedini, R.; Nasheghi, K. Q. Comparison of scaling equation with neural network model for prediction of asphaltene precipitation. *Journal of Petroleum Science and Engineering* **2010**, *72* (1-2), 186-194.
- (118) Jamialahmadi, M.; Ahmadi, K. A new scaling equation for modeling of asphaltene precipitation. In *Nigeria annual international conference and exhibition*, 2003; OnePetro.
- (119) Hu, Y.-F.; Chen, G.-J.; Yang, J.-T.; Guo, T.-M. A study on the application of scaling equation for asphaltene precipitation. *Fluid phase equilibria* **2000**, *171* (1-2), 181-195.
- (120) Syed, F. I.; AlShamsi, A.; Dahaghi, A. K.; Neghabhan, S. Application of ML & AI to model petrophysical and geo-mechanical properties of shale reservoirs—A systematic literature review. *Petroleum* **2020**.

(121) Mazloom, M. S.; Rezaei, F.; Hemmati-Sarapardeh, A.; Husein, M. M.; Zendehboudi, S.; Bemani, A. Artificial intelligence based methods for asphaltenes adsorption by nanocomposites: Application of group method of data handling, least squares support vector machine, and artificial neural networks. *Nanomaterials* **2020**, *10* (5), 890.

(122) Sayyad Amin, J.; Alamdari, A.; Mehranbod, N.; Ayatollahi, S.; Nikooee, E. Prediction of asphaltene precipitation: Learning from data at different conditions. *Energy & Fuels* **2010**, *24* (7), 4046-4053.

(123) Ahmadi, M. A.; Shadizadeh, S. R. New approach for prediction of asphaltene precipitation due to natural depletion by using evolutionary algorithm concept. *Fuel* **2012**, *102*, 716-723.

(124) Ahmadi, M. A. Neural network based unified particle swarm optimization for prediction of asphaltene precipitation. *Fluid Phase Equilibria* **2012**, *314*, 46-51.

(125) Qi, Z.; Abedini, A.; Sharbatian, A.; Pang, Y.; Guerrero, A.; Sinton, D. Asphaltene deposition during bitumen extraction with natural gas condensate and naphtha. *Energy & Fuels* **2018**, *32* (2), 1433-1439.

(126) Shahsavari, N.; Riazi, M.; Malayeri, M. Removal of asphaltene deposition in porous media using emulsified solvents-A visual study. *Journal of Petroleum Science and Engineering* **2020**, *191*, 107207.

(127) Zhang, J.; Tian, D.; Lin, M.; Yang, Z.; Dong, Z. Effect of resins, waxes and asphaltenes on water-oil interfacial properties and emulsion stability. *Colloids and Surfaces A: Physicochemical and Engineering Aspects* **2016**, *507*, 1-6.

(128) Chang, C.-C.; Williams, I.; Nowbahar, A.; Mansard, V.; Mecca, J.; Whitaker, K. A.; Schmitt, A. K.; Tucker, C. J.; Kalantar, T. H.; Kuo, T.-C. Effect of Ethylcellulose on the Rheology and Mechanical Heterogeneity of Asphaltene Films at the Oil–Water Interface. *Langmuir* **2019**, *35* (29), 9374-9381.

(129) Ma, J.; Li, X.; Zhang, X.; Sui, H.; He, L.; Wang, S. A novel oxygen-containing demulsifier for efficient breaking of water-in-oil emulsions. *Chemical Engineering Journal* **2020**, *385*, 123826.

(130) Ismail, I.; Kazemzadeh, Y.; Sharifi, M.; Riazi, M.; Malayeri, M. R.; Cortés, F. Formation and stability of W/O emulsions in presence of asphaltene at reservoir thermodynamic conditions. *Journal of Molecular Liquids* **2020**, *299*, 112125.

TOC graphic

